Structural and magnetic properties of sputter deposited Mn-Fe-Ga thin films

Alessia Niesen[1], Christian Sterwerf[1], Manuel Glas[1], Jan-Michael Schmalhorst[1] and Günter Reiss[1]

[1]Center for Spinelectronic Materials and Devices, Physics Department, Bielefeld University, Germany

arXiv:1511.02097v2 [cond-mat.mtrl-sci] 1 Aug 2016

***Abstract*—We investigated structural and magnetic properties of sputter deposited Mn-Fe-Ga compounds. The crystallinity of the Mn-Fe-Ga thin films was confirmed using x-ray diffraction. X-ray reflection and atomic force microscopy measurements were utilized to investigate the surface properties, roughness, thickness and density of the deposited Mn-Fe-Ga. Depending on the stoichiometry, as well as the used substrates ($SrTiO_3$ (001) and MgO (001)) or buffer layer (TiN) the Mn-Fe-Ga crystallized in the cubic or the tetragonally distorted phase. Anomalous Hall effect and alternating gradient magnetometry measurements confirmed strong perpendicular magnetocrystalline anisotropy. Hard magnetic behavior was reached by tuning the composition. TiN buffered $Mn_{2.7}Fe_{0.3}Ga$ revealed sharper switching of the magnetization compared to the unbuffered layers.**

***Index Terms*—Heusler compounds, perpendicular magnetocrystalline anisotropy, material science, spintronics**

I. Introduction

Ferromagnetic, fully spin polarized materials (half-metals) found a lot of interest in the recent years due to their possible application in spintronic devices as nonvolatile memories [1] and field programmable logic devices. [2], [3] To maintain the thermal stability at shrinking device sizes, an out-of-plane (oop) oriented magnetization of the material is advantageous. Therefore investigation of perpendicularly magnetized Heusler compounds has found attraction. High spin polarization and out-of-plane magnetization direction was predicted for the $Mn_{3-x}Ga$ ($0.15 \leq x \leq 2$) compound. [4]–[6] The transition from the cubic $D0_3$ into the tetragonal $D0_{22}$ phase takes place at temperatures above 500°C. [7] Hence a variation of the deposition temperature is an important criterium in terms of the crystallographic properties. The tetragonally distortion could also be obtained by shifting the Fermi energy at the Van Hove singularity in one of the spin-channels, which is reached by tuning the material with an additional element. [8] Mn-Fe-Ga is one possible material, which is calculated to be $95\,\%$ spin polarized at the Fermi level for the cubic phase (Mn_2Fe_1Ga). [9] The predicted low total magnetization $M = 1.03\,\mu_B$ [9] and high Curie temperature $T_C = 550\,\mathrm{K}$ (lowest measured value for $Mn_{1.4}Fe_{1.6}Ga$) makes this material interesting to serve as an electrode in magnetic tunnel junctions (MTJ's). [10] The replacement of Mn atoms by Fe leads to an enhancement of the magnetic moment. The measured magnetic moment of pure Mn-Ga (prepared by arc melting) is $1\,\mu_B$. The Fe - rich Fe_2Mn_1Ga showed the highest magnetic moment of $3.5\,\mu_B$. [10]

The tunable magnetic behavior makes this material interesting for investigations and a promissing candidate for applications. In this work, we focused on the preparation and investigation of the crystallographic, structural and magnetic properties of the ternary Mn-Fe-Ga compound thin films. The influence of different stoichiometries, substrates and deposition temperatures on the material properties was analyzed. With regard to the preparation of magnetic tunnel junctions and the aim to increase their applicability, additionally a TiN seed-layer was used. Sputter deposited TiN is a material with low electrical resistivity ($16\,\mu\Omega\,\mathrm{cm}$) and a surface roughness below $1\,\mathrm{nm}$. [11], [12] Thus it provides a good electrical connection to the MTJ. High thermal stability (melting point $2950\,^\circ\mathrm{C}$ [13]) is another advantage, which prevents chemical reactions of TiN with the on top deposited material. The lattice constant of TiN (fcc structure) is $4.24\,\text{Å}$ and therefore suitable for various Heusler compounds. It was already shown, that TiN is a suitable seed-layer for $Mn_{3-x}Ga$ and Co_2FeAl. [14]

II. Experimental

Mn-Fe-Ga thin films ($40\,\mathrm{nm}$ thickness) were prepared in an ultra-high-vacuum (UHV) sputtering system with a base pressure below $5 \times 10^{-10}\,\mathrm{mbar}$. DC magnetron co-sputtering from a pure Mn, Fe and a $Mn_{45}Ga_{55}$ composite target was used to prepare the samples. The Ar pressure was set to $1.7 \times 10^{-3}\,\mathrm{mbar}$. The amount of Mn, in the Mn_yFe_xGa compound, was varied in the range of $1.5 \leq y \leq 3$ and the amount of Fe in the range of $0.3 \leq x \leq 1$. Deposition temperatures from $190\,^\circ\mathrm{C}$ to $595\,^\circ\mathrm{C}$ were chosen in order to achieve crystalline growth and the tetragonally distorted phase of Mn-Fe-Ga. MgO (100) ($a_{\mathrm{MgO}} = 4.21\,\text{Å}$) and $SrTiO_3$ (STO) (100) ($a_{\mathrm{STO}} = 3.91\,\text{Å}$) single crystalline substrates were utilized. Additionally TiN buffered Mn-Fe-Ga thin films on MgO and STO substrates were prepared. The TiN layers ($30\,\mathrm{nm}$) were deposited using reactive sputtering in an Ar and N atmosphere which results in stoichiometric Ti_1N_1 thin films. During the sputtering process a N flow of $2\,\mathrm{sccm}$ and an Ar flow of $20\,\mathrm{sccm}$ was used, leading to a deposition pressure of $1.6 \times 10^{-3}\,\mathrm{mbar}$. The stoichiometry of TiN was verified via density, resistivity and x-ray absorption spectroscopy measurements. Additionally the superconductance of TiN was proved. Further information on the TiN seed-layer is given in [14]. On top of the Heusler compound a $2\,\mathrm{nm}$ thick MgO layer was deposited to prevent the surface from contaminations.

III. Characterization of the Mn-Fe-Ga compound

A. Crystal structure

Crystallographic and structural properties of the Mn-Fe-Ga thin films were determined via x-ray diffraction (XRD) and

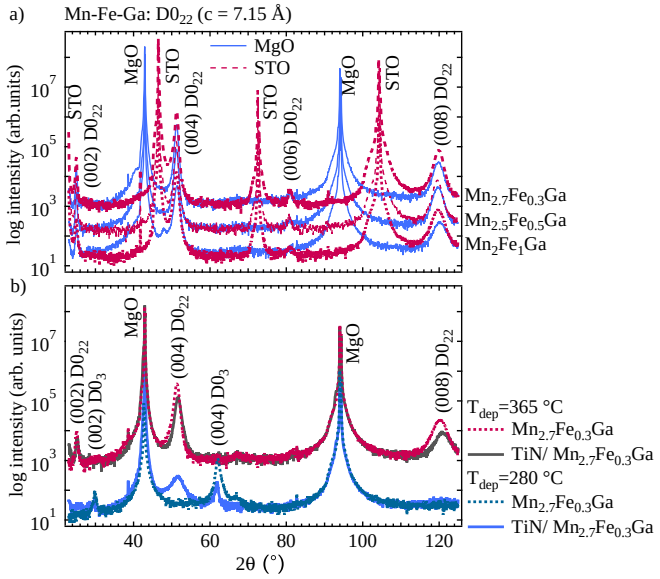

Fig. 1. a) XRD patterns of the $Mn_{3-x}Fe_xGa$ compound deposited at 450 °C on MgO (blue curves) and $SrTiO_3$ (dashed red curves) substrates. b) XRD patterns of $Mn_{2.7}Fe_{0.3}Ga$ deposited at 365 °C and 280 °C with and without a TiN buffer layer.

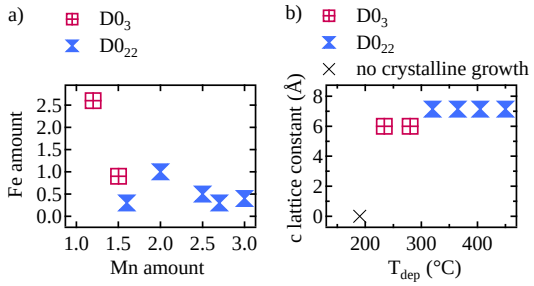

Fig. 2. a) Crystal structure of the Mn-Fe-Ga compounds deposited on MgO substrates in dependence on the Mn and Fe amount. b) Dependence of the crystal structure of $Mn_{2.7}Fe_{0.3}Ga$ on the deposition temperature.

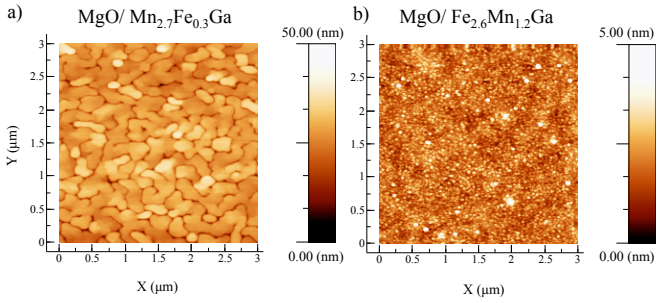

Fig. 3. AFM images of a) $Mn_{2.7}Fe_{0.3}Ga$ (tetragonally distorted phase) and b) $Fe_{2.6}Mn_{1.2}Ga$ (cubic phase) thin films deposited on MgO (100) substrates at 450 °C.

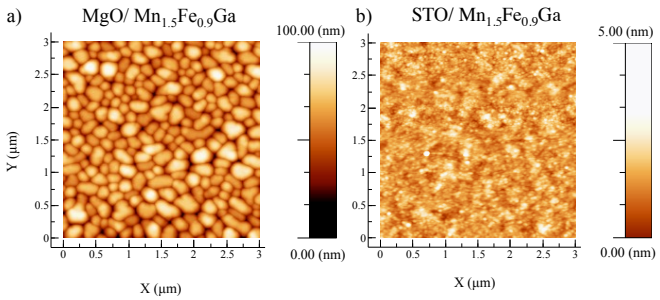

Fig. 4. AFM images of $Mn_{1.6}Fe_{0.9}Ga$ (tetragonally distorted) deposited on a) MgO (100) and b) STO (100) substrates at 550 °C.

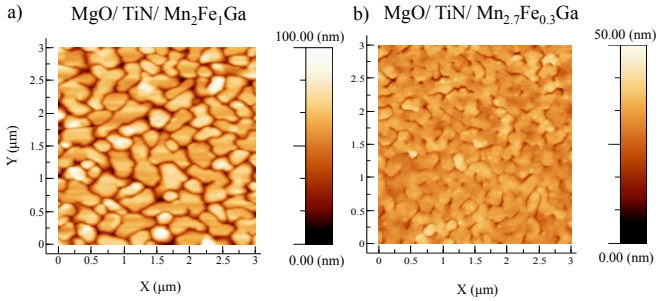

Fig. 5. AFM images of TiN buffered a) Mn_2Fe_1Ga and b) $Mn_{2.7}Fe_{0.3}Ga$ deposited on MgO (100) at 450 °C.

x-ray reflection (XRR) measurements using a XRD Philips X'Pert Pro diffractometer (Cu anode). The lowest roughness values ($\leq$ 1 nm) combined with the highest crystallinity were measured on samples deposited at temperatures of 407 °C and 450 °C. All samples with the $Mn_{3-x}Fe_xGa$ ($0.3 \leq x \leq 1$) stoichiometry crystallize in the D0$_{22}$ tetragonally distorted phase (Fig. 1 and Fig. 2) which is in good agreement with the previously reported data. [10] The determined in-plane and oop lattice constants are a = 3.9±0.01 Å and c = 7.15±0.04 Å for Mn-Fe-Ga deposited on both substrate types, leading to a c/a ratio of 1.8. The substrate type obviously does not influence the crystallographic phase of the $Mn_{3-x}Fe_xGa$. Therefore this stoichiometry is stabilized in the tetragonally distorted phase. Increasing the Fe and decreasing the Mn amount leads to a formation of the cubic phase (D0$_3$) (c = 6 Å) on MgO substrates (Fig. 2). On STO each composition results in a formation of the tetragonally distorted phase, due to the low lattice mismatch of 0.5% with the in-plane lattice constant. The dependence of the crystal structure on the deposition temperature was investigated for the $Mn_{2.7}Fe_{0.3}Ga$ compound, which showes the tetragonally distortion on each substrate type, as well as on the TiN buffer layer. The transition from the cubic D0$_3$ ($a = c = 6$ Å) into the tetragonally distorted D0$_{22}$ phase takes place at a deposition temperature of 320 °C (Fig. 2). The density of the samples was determined via XRR measurements and also revealed a dependence on the crystallographic phase. The density of the tetragonally distorted Mn-Fe-Ga is 7.1±0.5 g/cm^3 and 6±0.5 g/cm^3 for the cubic phase.

Deposition on a TiN buffer layer ($a_{TiN} = 4.24$ Å) leads to a mixture of the cubic D0$_3$ and the D0$_{22}$ phase, depending on the Mn-Fe-Ga composition and the deposition temperature. The tetragonally distorted phase for the $Mn_{2.7}Fe_{0.3}Ga$, on a TiN seed-layer, appears already at a deposition temperature of 280 °C (Fig. 1), which is a lower temperature compared to the unbuffered sample. The seed-layer obviously influences

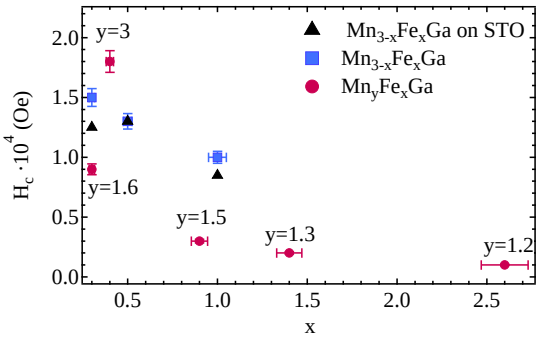

Fig. 6. Coercivity dependence on the stoichiometry of Mn-Fe-Ga deposited on MgO and STO substrates. The blue squaress and black triangles give the coercivity values for $Mn_{3-x}Fe_xGa$. The red circles point out the values for the Mn_yFe_xGa stoichiometries (y gives the values for the amount of Mn).

the crystalline growth of this compound leading to a lower deposition temperature at which the tetragonally distorted phase is formed. We already observed this behavior for the Mn-Ga compound. [14] TiN buffered $Mn_{2.5}Fe_{0.5}Ga$ forms a mixture of the cubic and the tetragonally distorted phase. In case of TiN buffered Mn_2Fe_1Ga, only the cubic phase was formed.

B. Surface properties

Atomic force microscopy (AFM) was carried out to investigate the surface topography of the samples. Fig. 3 shows a comparison of (a) the tetragonally distorted $Mn_{2.7}Fe_{0.3}Ga$ and (b) the cubic $Fe_{2.6}Mn_{1.2}Ga$ layer deposited on MgO at 450 °C. The $Mn_{2.7}Fe_{0.3}Ga$ forms 200 nm - 400 nm broad grains with steep grain boundaries. The measured rms roughness value is 3.4 ± 0.05 nm. The cubic $Fe_{2.6}Mn_{1.2}Ga$ compound forms small grains and a smooth surface (roughness = 0.8 ± 0.05 nm). Mn-Fe-Ga with lower Mn ratio shows island growth (Fig. 4 a). The obtained roughness value is 17 ± 0.5 nm. The equivalent film (temperature and stoichiometry) on STO revealed no island growth and low roughness of 0.43 ± 0.05 nm (Fig. 4 b), which can be attributed to the low lattice mismatch with the in-plane lattice constant of the tetragonally distorted Mn-Fe-Ga.

We indicate that the applied roughness analysis is leading to an overestimation of the roughness for samples, which consist of big grains with steep grain boundaries. The structure of Mn-Fe-Ga deposited on a TiN seed-layer also showed a strong dependence on the stoichiometry. As previously mentioned, TiN buffered Mn_2Fe_1Ga crystallizes in the cubic $D0_3$ phase. Due to the high lattice mismatch of the cubic phase with the lattice constant of TiN (8.3%) island growth and high roughness (14.25 ± 0.05 nm) appears (Fig. 5 a). The TiN buffered $Mn_{2.7}Fe_{0.3}Ga$, crystallized in the $D0_{22}$ phase, shows a similar morphology and roughness value as the unbuffered sample (Fig. 3 a) and (Fig. 5 b). Without a TiN buffer layer we determined a roughness value of 3.4 ± 0.05 nm (see above) compared to 3.54 ± 0.05 nm with a TiN buffer.

C. Magnetic properties

The magnetic properties were investigated via AGM (alternating gradient magnetometry) and AHE (anomalous Hall effect) measurements. The coercivity of the Mn-Fe-Ga thin films was determined via AHE measurements in a 4-terminal arrangement, carried out in a closed cycled He-cryostat. High coercivity fields ($H_c \leq 2\times10^4$ Oe) in the oop direction can be reached by tuning the composition. The coercivity decreases with increasing Fe and decreasing Mn amount for both substrate types. The highest coercivity of 1.8×10^4 Oe was measured for $Mn_3Fe_{0.4}Ga$. The lowest value of 0.2×10^4 Oe showed the cubic $Mn_{1.3}Fe_{1.4}Ga$ (Fig. 6). Each sample revealed a hard magnetic axis in the in-plane direction. Since the samples could not be saturated in the in-plane direction even at an applied field of 4×10^4 Oe, a strong perpendicular magnetocrystalline anisotropy (PMA) could be experimentally verified. Fig. 7 shows a comparison of normalized magnetization M and AHE curves (U_H) for the tetragonally distorted Mn-Fe-Ga deposited on STO (smooth films with roughness values below 1 nm). In case of the $Mn_{1.2}Fe_{2.6}Ga$ and $Mn_{1.5}Fe_{0.9}Ga$ deposited on STO substrates the hysteresis curves are in good agreement. The coercivity, the squareness ratio and the saturation magnetization values are given in Tab. I. We defined the squareness as $S_R = M_r/M_s$ or $S_R = \rho_{yx_r}/\rho_{yx_s}$ (the r or s index denotes the remanence or the saturation value of the magnetization M or resistivity ρ). Increasing the Mn and lowering the amount of Fe obviously also leads to an increase of the squareness ratio. The magnetization values, determined via AGM measurements, are in the range of 140 kA/m and 350 kA/m, which is comparable to the values of the Mn-Ga compound. [15] $Mn_{1.6}Fe_{0.3}Ga$ shows a feature in the AGM curves around 0 Oe field, which could not be observed via AHE measurements. This was attributed to a second phase

sample	H_c (Oe)	S_R	M_S (kA/m)
$Mn_{1.2}Fe_{2.6}Ga$	0.1×10^4	0.5	144 ± 14
$Mn_{1.5}Fe_{0.9}Ga$	0.3×10^4	0.95	350 ± 10
$Mn_{1.6}Fe_{0.3}Ga$	0.9×10^4	0.97	317 ± 13

TABLE I
COERCIVITY H_c, SQUARENESS RATIO S_R AND SATURATION MAGNETIZATION M_S VALUES OF MN-FE-GA DEPOSITED ON STO DETERMINED VIA AHE AND AGM MEASUREMENTS.

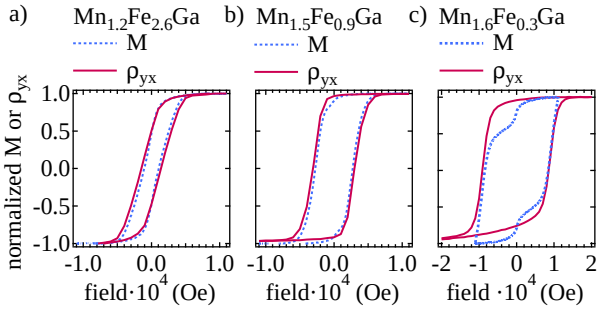

Fig. 7. oop measured AHE (red) and AGM (dashed blue) hysteresis curves for a) $Mn_{1.2}Fe_{2.6}Ga$, b) $Mn_{1.5}Fe_{0.9}Ga$ and c) $Mn_{1.6}Fe_{0.3}Ga$ thin films deposited on STO. The measured magnetization M and Hall voltage values U_H are normalized for a better comparison.

T_{dep}=365 °C	H_c (Oe)	S_R
w/o TiN	1.4×10^4	0.53
w TiN	1.2×10^4	0.93
T_{dep}=450 °C		
w/o TiN	1.5×10^4	0.74
w TiN	1.2×10^4	0.98

TABLE II
COMPARISON OF THE COERCIVITY AND SQUARENESS RATIO VALUES OF TIN BUFFERED (W TIN) AND UNBUFFERED (W/O TIN) $Mn_{2.7}Fe_{0.3}Ga$ DEPOSITED ON MGO SUBSTRATES.

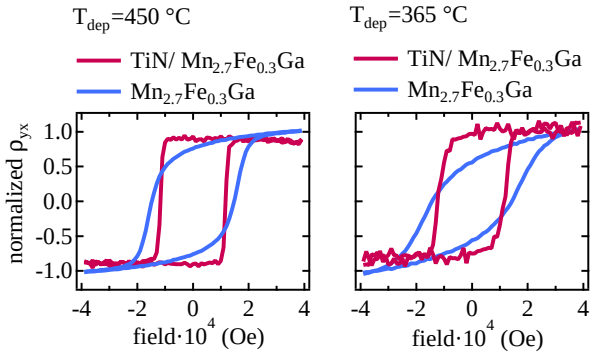

Fig. 8. AHE hysteresis curves of TiN buffered (red) and unbuffered (blue) Mn-Fe-Ga measured at room temperature. Both samples were deposited on MgO substrates. The TiN seed-layer (30 nm thickness) was deposited at 405 °C. The $Mn_{2.7}Fe_{0.3}Ga$ thin films were deposited at 450 °C and 365 °C, respectively.

(soft magnetic) inside the Mn-Fe-Ga thin film, which has a different coercive field. Such behavior was already observed for Mn_2Fe_1Ga samples. [16] The AHE measurements do not show such a feature, which indicates that the second phase could have a high resistance and therefore does not contribute to the AHE. A second phase was not detected via XRD measurements, leading to the assumption that this phase is an amourphous part of the material, which might be located at the grain boundaries. To increase the applicability of Mn-Fe-Ga as an electrode in MTJ's a TiN seed-layer (30 nm thickness) was used. Fig. 8 shows a comparison of the AHE mesurements for TiN buffered $Mn_{2.7}Fe_{0.3}Ga$ deposited at two different temperatures. In both cases the TiN buffered samples revealed sharper switching of the magnetization compared to the unbuffered layers. The squareness ratio increases and the coercive field decreases for the buffered samples (Tab. II). Regarding the similar morphology of the samples, the reason for the changed switching behavior is still unclear and we attempt further investigations on this topic.

IV. CONCLUSION

Structural and magnetic properties of sputter deposited Mn-Fe-Ga compounds were investigated. Depending on the stoichiometry, the deposition temperature, as well as the used substrate (STO (001) and MgO (001)) or buffer layer (TiN) the Mn-Fe-Ga crystallizes in the cubic $D0_3$ (c = 6 Å) or the tetragonally distorted phase $D0_{22}$ (c = 7.15 Å). The main drawback for applications is the island growth, which was confirmed via AFM measurements. Low roughness ($\leq$ 1 nm) and the $D0_{22}$ phase was observed for each used deposition temperature and composition of the Mn-Fe-Ga on STO, whereas on MgO substrates the roughness showed strong dependence on the deposition temperature and the Mn-Fe-Ga composition. Strong PMA was confirmed via AHE and AGM measurements. High coercivity fields (up to $H_c \leq 2 \cdot 10^4$ Oe) in the out-of-plane direction were reached by tuning the composition. TiN buffered $Mn_{2.7}Fe_{0.3}Ga$ revealed sharper switching of the magnetization compared to the unbuffered layers. Similar results were achieved for TiN buffered Mn-Ga and Co_2FeAl thin films. [14]

ACKNOWLEDGMENTS

The authors gratefully acknowledge financial support by the Deutsche Forschungsgemeinschaft (DFG, Contract No. RE 1052/32-1).

APPENDIX A

The roughness values (root mean square) were calculated using a standard deviation of surface heights:

$$RMS = \sqrt{\frac{1}{N}\Sigma_{x=1}^{N}(z(x,y) - \overline{z}(N,M))^2} \qquad (1)$$

with $\overline{z}(N,M)$ the arithmetic average height. The surface is described by a matrix with N lines and M columns corresponding to the points (x,y) of the height z(x,y).

REFERENCES

[1] S. A. Wolf, *Science*, vol. 294, no. 5546, p. 1488, 2001.
[2] G. Reiss and D. Meyners, *Journal of Physics: Condensed Matter*, vol. 19, no. 16, p. 165220, 2007.
[3] A. Thomas, D. Meyners, D. Ebke, N.-N. Liu, M. D. Sacher, J. Schmalhorst, G. Reiss, H. Ebert, and A. Hütten, *Applied Physics Letters*, vol. 89, no. 1, p. 012502, 2006.
[4] B. Balke, G. H. Fecher, J. Winterlik, and C. Felser, *Applied Physics Letters*, vol. 90, no. 15, p. 152504, 2007.
[5] J. Winterlik, B. Balke, G. Fecher, C. Felser, M. Alves, F. Bernardi, and J. Morais, *Physical Review B*, vol. 77, no. 5, p. 12, 2008.
[6] S. Wurmehl, H. C. Kandpal, G. H. Fecher, and C. Felser, *Journal of Physics: Condensed Matter*, vol. 18, no. 27, p. 6171, 2006.
[7] M. Glas, C. Sterwerf, J.-M. Schmalhorst, D. Ebke, C. Jenkins, E. Arenholz, and G. Reiss, *Journal of Applied Physics*, vol. 114, no. 18, p. 183910, 2013.
[8] J. Winterlik, S. Chadov, A. Gupta, V. Alijani, T. Gasi, K. Filsinger, B. Balke, G. H. Fecher, C. A. Jenkins, F. Casper, J. Kübler, G.-D. Liu, L. Gao, S. S. P. Parkin, and C. Felser, vol. 24, no. 47, p. 6283, 2012.
[9] L. Wollmann, S. Chadov, J. Kübler, and C. Felser, *Physical Review B*, vol. 90, no. 21, p. 214420, 2014.
[10] C. Felser, V. Alijani, J. Winterlik, S. Chadov, and A. K. Nayak, *IEEE Transactions on Magnetics*, vol. 49, no. 2, p. 682, 2013.
[11] F. Magnus, A. S. Ingason, S. Olafsson, and J. T. Gudmundsson, *Thin Solid Films*, 2011.
[12] Y. Krockenberger, S.-i. Karimoto, H. Yamamoto, and K. Semba, *Journal of Applied Physics*, vol. 112, no. 8, p. 083920, 2012.
[13] M. Pritschow, "Titannitrid- und titan-schichten für die nano-elektromechanik," Ph.D. dissertation, Institut für Mikroelektronik Stuttgart, Mechanical Engineering Department, 2007.
[14] A. Niesen, M. Glas, J. Ludwig, J.-M. Schmalhorst, R. Sahoo, D. Ebke, E. Arenholz, and G. Reiss, *Journal of Applied Physics*, vol. 118, no. 24, p. 243904, 2015.

[15] M. Glas, D. Ebke, I. M. Imort, P. Thomas, and G. Reiss, *Journal of Magnetism and Magnetic Materials 333*, p. 134, 2013.
[16] T. Gasi, A. K. Nayak, J. Winterlik, V. Ksenofontov, P. Adler, M. Nicklas, and C. Felser, *Applied Physics Letters*, vol. 102, no. 202402, 2013.